

Chapter 41

Pan-Sharpening Techniques to Enhance2

Archaeological Marks: An Overview3

Rosa Lasaponara and Nicola Masini4

Abstract The application of pan-sharpening techniques to very high resolution 5
(VHR) satellite data can fruitfully improve the enhancement of archaeological 6
marks and facilitate their detection. Nevertheless, the quantitative evaluation of 7
the quality of the fused images is one the most crucial aspects in the context of data 8
fusion. This is because (i) data fusion application is a rather recent technique 9
applied to archaeology; (ii) the criteria generally adopted for the data fusion 10
evaluation can not fit the needs of this type of application. This chapter provides 11
an overview of pan-sharpening techniques and quantitative evaluation of their 12
capability in (i) preserving spectral fidelity and (ii) sharpening spatial and textural 13
content.14

Keywords Pan-sharpening • Assessment criteria • Very high resolution • 15
Archaeological marks16

4.1 Introduction17

The use of pan-sharpening techniques enables the integration of the complementary 18
information acquired from the panchromatic and multispectral (MS) imaging 19
sensors. The higher spatial resolution of the panchromatic can be suitably merged 20
with the spectral capability of multispectral channels.21

R. Lasaponara (✉)
Institute of Methodologies for Environmental Analysis, CNR-IMAA,
C. da S. Loya, 85100 Tito Scalo, Potenza, Italy
e-mail: lasaponara@imaa.cnr.it

N. Masini
Institute of Archaeological and Architectural Heritage, CNR-IBAM,
C. da S. Loya, 85050 Tito Scalo, Potenza, Italy
e-mail: n.masini@ibam.cnr.it

Over the years, a number of algorithms have been developed for data fusion, among them we will focus on the most widely used: Intensity-Hue-Saturation (IHS), Principal Component Analysis (PCA), different arithmetic combination (e.g., Brovey transform), Zhang algorithm, high-pass filtering, Ehlers algorithm, multi-resolution based methods (e.g., pyramid algorithm, wavelet transform), and Artificial Neural Networks (ANNs).

The evaluation and numerical comparisons of the diverse pan-sharpening algorithms is quite complex. Several statistical indicators have been designed for assessing the performance of image fusion algorithms in terms of preserving both: (i) spectral fidelity and (ii) spatial and textural content. In this chapter we focus on the specific requirements necessary for the enhancement of archaeological features through pan-sharpening techniques as well as on the evaluation of their performance.

4.2 Data Fusion in Remote Sensing for Archaeology

The use of data fusion techniques can fruitfully improve the enhancement of archaeological marks and make their detection easier by exploiting jointly the higher spatial resolution of the panchromatic image and the multispectral properties of the spectral channels (Fig. 4.1). Moreover, another advantage of using data fusion products is that the increased spatial resolution can fruitfully provide a

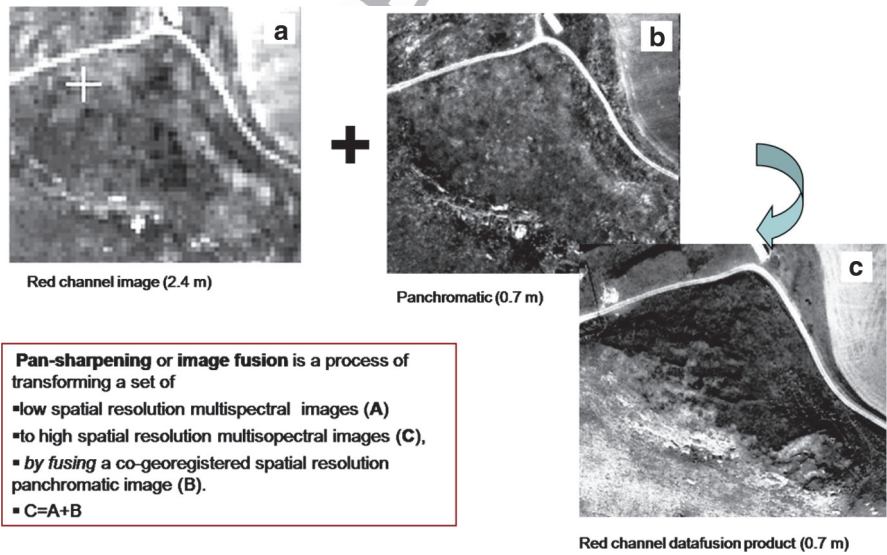


Fig. 4.1 Pan-sharpening allows us to exploit the higher spatial resolution of the panchromatic image and the multispectral properties, thus improving the enhancement of archaeological features

more accurate localization of the archaeological features. This more accurate localization, from the initial spatial resolution of multispectral data around meter (2.4 m for QuikBird, 2 m for GeoEye) to the sub-meters spatial resolution of panchromatic (0.6 m for QuickBird or 0.5 m for GeoEye) can be very helpful during in situ survey, such as GPS (Global Position System) campaigns, geophysical prospection or excavation trials.

Nevertheless, in order to take advantages from data fusion techniques, it is mandatory to quantitatively evaluate the benefits of different algorithms and approaches (Alparone et al. 2007). The quantitative evaluation of the quality of the fused images is yet one of the most crucial aspects in the context of data fusion. This issue is particularly relevant in the case of the identification of archaeological marks, because (i) data fusion application is a rather recent topic approached in the field of remote sensing of archaeology (Lasaponara and Masini 2007; Aiazzi et al. 2008; Lasaponara et al. 2008); (ii) the criteria generally adopted for the data fusion evaluation cannot fit the needs of remote sensing archaeology that are mainly focused on the identification of small features, that can be easily obscured by noise.

The best results from data fusion is that the multispectral set of fused images should be as identical as possible to the set of multispectral images that the corresponding sensor (Alparone et al. 2007; Aiazzi et al. 2008; Lasaponara et al. 2008) would observe with the high spatial resolution of panchromatic.

As no multispectral reference images are available at the requested higher spatial resolution, the assessment of the quality of the fused products is not obvious. Several score indices or figure metrics have been designed over the years (see Thomas and Wald 2004) to evaluate the performances of the fused images. Both intra-band indices and inter-band indices have been set up in order to measure respectively, spatial distortions (radiometric and geometric distortions) and spectral distortions (colour distortions).

In order to assess the performance of data fusion algorithms, three properties should be verified as expressed by Wald et al. (1997): (1) the data fusion products, once degraded to their original resolution, should be equal to the original; (2) the data fusion image should be as identical as possible to the MS image that would be acquired by the corresponding sensor with the high spatial resolution of the Pan sensor; (3) the MS set of fused images should be as identical as possible to the set of MS images that would be acquired by the corresponding sensor with the high spatial resolution of Pan.

As no multispectral reference images are available at the requested higher spatial resolution, the verification of the second and the third property is not obvious. In order to overcome this drawback, diverse methodological approaches can be used: (i) the Wald protocol (Wald et al. 1997), (ii) the Zhou protocol (Zhou et al. 1998), and, finally, (iii) the QNR (Quality with No Reference) index devised by Alparone et al. (2007). In Sect. 3 we provide an overview of the currently available pan-sharpening techniques and in Sect. 4 detail for their numerical evaluation.

4.3 Overview on Pan-Sharpening Techniques

Pan-sharpening is a branch of image fusion that is receiving ever increasing attention from the remote sensing community for multiple applications in different fields such as pattern recognition, visual enhancement, classification, change detection, object detection and area surveillance (Pohl and Van Genderen 1998).

New-generation space-borne imaging sensors operating in a variety of ground scales and spectral bands provide huge volumes of data having complementary spatial and spectral resolutions. Constraints on the signal to noise ratio (SNR) impose that the spatial resolution must be lower, if the desired spectral resolution is larger. Conversely, the highest spatial resolution is obtained whenever no spectral diversity is required. The trade-off of spectral and spatial resolution makes it desirable to perform a spatial enhancement of the lower resolution multi-spectral (MS) data or, equivalently, to increase the spectral resolution of the data-set having a higher ground resolution, but a lower spectral resolution; as a limit case, constituted by a unique panchromatic image (Pan) bearing no spectral information.

According to Jiang Dong et al. 2009, pan-sharpening may be obtained at different levels, which are categorized as follow: (i) signal level, (ii) pixel level, (iii) feature level, and (iv) decision level as follows (see Fig. 4.2):

- (1) Signal level fusion algorithms elaborate signals acquired from different sensors to create a new signal characterized by an improved signal-to noise ratio respect to that of the original signals.
- (2) Pixel level fusion algorithms elaborate information on a pixel-by-pixel basis to create a fused image from a set of pixels in original images to improve features visibility and results from image processing tasks such as segmentation, classification, etc
- (3) Feature level fusion algorithms elaborate information on feature level after the recognition and extraction of objects from pixel intensities, edges or textures in the original data sources.
- (4) Decision-level fusion algorithms elaborate information at a higher level of abstraction, namely information extraction is carried out using results from multiple algorithms which are then combined using given decision rules.

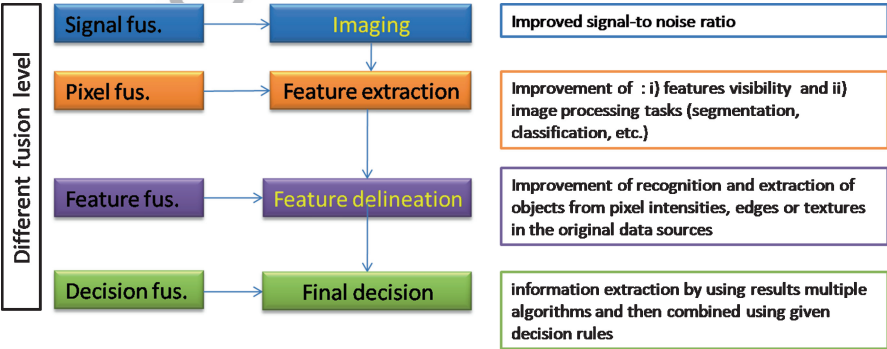


Fig. 4.2 Pan-sharpening categorization

Over the years numerous image fusion techniques have been developed. 116
Among them we will focus on the most widely used: intensity-hue-saturation (IHS), 117
principal component analysis (PCA), different arithmetic combination (e.g. Brovey 118
transform), Zhang, high-pass filtering, Ehlers, multi-resolution analysis-based methods 119
(e.g., pyramid algorithm, wavelet transform), and Artificial Neural Networks (ANNs). 120

These methods are based on the following general protocol: the high-resolution 121
geometrical information of the Pan scene is extracted and incorporated into the low- 122
resolution MS images, by a proper modelling of the relationships between the Pan 123
and MS bands. 124

In general, the image fusion methods can be divided into these three main classes 125
depending on how the spatial details are extracted from the Pan image: 126

- (i) techniques based on arithmetic combinations of multispectral images 127
resampled at the higher spatial resolution of Pan; 128
- (ii) component substitution (CS) techniques based on a spectral transformation of 129
the MS data followed by replacement of the first transformed component with 130
the Pan image. Later a reverse transformation is carry out to yield back the 131
sharpened MS bands; 132
- (iii) techniques that employ multi-resolution analysis (MRA) to extract the geo- 133
metrical information that will be added to the MS bands, from the Pan image. 134

4.4 Pan-Sharpening Techniques Based on Arithmetic 135 Combinations 136

The simplest approach for fusing the Pan and MS images is based on arithmetic 137
combinations of different scenes performed at the pixel level. This approach is 138
generally obtained through two computation steps: 139

- (I) Re-sampling of the selected spectral bands to the panchromatic spatial 140
resolution; 141
- (II) selection and application of the arithmetic combinations, which span from the 142
simple multiplication, to Brovey transformation, Synthetic Variable Ratio 143
(SVR), and Ratio Enhancement 144

4.4.1 Multiplicative Approach Fusion 145

This algorithm is one of the simplest pan-sharpening algorithms being only based 146
on the multiplication of each multispectral band with the panchromatic image. The 147
image fusion is carried out as follows: 148

- (i) selection of spectral bands and resampling to panchromatic spatial resolution; 149
- (ii) application of multiplication to obtain the transformation 150

$$Fusion_k = Multi_k \times Pan \quad (4.1)$$

151 $Fusion_k$ is the k th fused multispectral band, $Multi_k$ is the k th original MS image
152 resampled to the Pan spatial resolution.

153 The advantages of the multiplicative approach are the following: (i) it does alter
154 the spectral characteristics of the original image data, (ii) it is simple and quite fast

155 **4.4.2 Brovey Transformation**

156 Brovey equation is designed on the basis of the assumption that spectral range of the
157 panchromatic image is the same as that covered by the multispectral data. The
158 transformation is defined by the following equation:

$$Fusion_k = \frac{Multi_k}{Multi_{sum}} \times Pan \quad (4.2)$$

159 $Fusion_k$ is the k th fused MS band, $Multi_k$ is the k th original MS image, $Multi_{sum}$
160 is a synthetically panchromatic image obtained by the sum of MS bands at the same
161 resolution as the original MS images.

162 The image fusion is carried out as follows:

- 163 (i) selection of spectral bands and resampling to panchromatic spatial resolution;
- 164 (ii) application of Brovey transformation.

165 Brovey transformation is implemented in the most popular image processing
166 software such as PCI ENVI, ERDAS, etc.

167 **4.4.3 Synthetic Variable Ratio (SVR) and Improved-SVR**

168 The SVR pan-sharpening method (Munechika et al. 1993) is based on Eq. 4.3

$$Fusion_k = \frac{Multi_k}{Pan_{syn}} \times Pan \quad (4.3)$$

169 $Fusion_k$ is the k th fused multispectral band, $Multi_k$ is the k th original MS image,
170 Pan_{syn} is a synthetically panchromatic image obtained at the same resolution as the
171 original MS images by Suits et al. (1988) equation:

$$Pan_{syn} = \sum_{i=1}^4 \varphi_i X S_{Li} \quad (4.4)$$

172 The parameters φ_i are only computed for some typical land cover types: (i) urban,
173 (ii) soil, (iii) water, (iv) trees and (v) grass using a regression analysis between

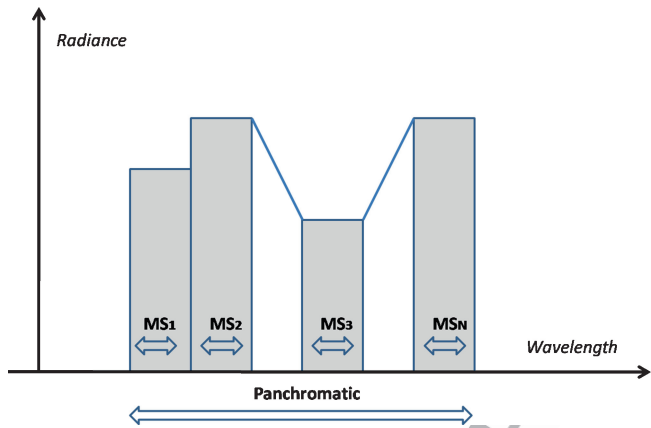


Fig. 4.3 Computation scheme of Wang et al. 2008 algorithm

the values simulated through a given atmospheric model and those measured. The histogram matching was used to force the original Pan image to the PanSyn.

Zhang (2004) developed a data fusion algorithm specifically devised for VHR satellite images and mainly based on the computation of the parameters φ_i using a multiple regression analysis instead of only consider the five main land covers listed before (urban, soil, water, trees and grass).

According to Zhang (2004), this statistics-based fusion technique may solve the two major problems in image fusion: (i) color distortion and (ii) operator (or dataset) dependency the following ways:

- (1) the reduction of the color distortion is obtained through least squares technique to find the best fit between the grey values of the image bands being fused and to adjust the contribution of individual bands to the fusion result;
- (2) the elimination of dataset dependency is carry out by employing a set of statistic approaches to estimate the grey value relationship between all the input bands

This algorithm is available in a PCI-Geomatics routine (PANSHARP). In the PANSHARP routine, if the original MS and Pan images are geo-referenced, the resampling process can also be accomplished together with the fusion within one step. All the MS bands can be fused at one time. The fusion can also be performed solely on user-specified MS bands.

Wang et al. 2008, developed an improved synthetic variable ratio method for image fusion, mainly based on the assumption that the radiance of the synthesized panchromatic band can be obtained integrating the radiance of MS bands under the hypothesis that the panchromatic band covers exactly the same range as the MS bands to be processed. Therefore, in these conditions, the radiance of the synthesized panchromatic images can be obtained as the integral. The computation is arranged in this way (see Fig. 4.3):

- (i) the radiance of each MS band is assumed as equal to the rectangular area;

- 201 (ii) regarding the gap between the spectral bands, the radiance is obtained as the
202 area of the trapezoid areas between the rectangles;
203 (iii) finally, the integral is obtained by summing all the areas together.

204 **4.5 Pan-Sharpening Techniques Based**
205 **on Component Substitution**

206 Pan-sharpening Component Substitution (CS) is a typology of simple and fast
207 technique based on a spectral transformation of the original bands in a new
208 vector space. Most widely used transformations are Intensity-Hue-Saturation
209 (IHS), Principal Component Analysis (PCA; see Richards and Jia 2006 and Sect.
210 2.3.4.2 in this book), and Gram-Schmidt orthogonalisation procedure (Laben et al.
211 2000; Aiazzi et al. 2007).

212 The rationale of CS fusion is that one of the transformed components (usually
213 the first component or *intensity*, I_L) is *substituted* by the high-resolution Pan image,
214 P , before the inverse transformation is applied.

215 **4.5.1 Principal Component Analysis Pan-Sharpening**

216 In pan-sharpening based on PCA (Chavez et al. 1991), the PAN image replaces the
217 first principal component. Prior to the substitution, the PAN image is stretched such
218 that its mean and variance are similar to that of the first principal component
219 (Fig. 4.4).

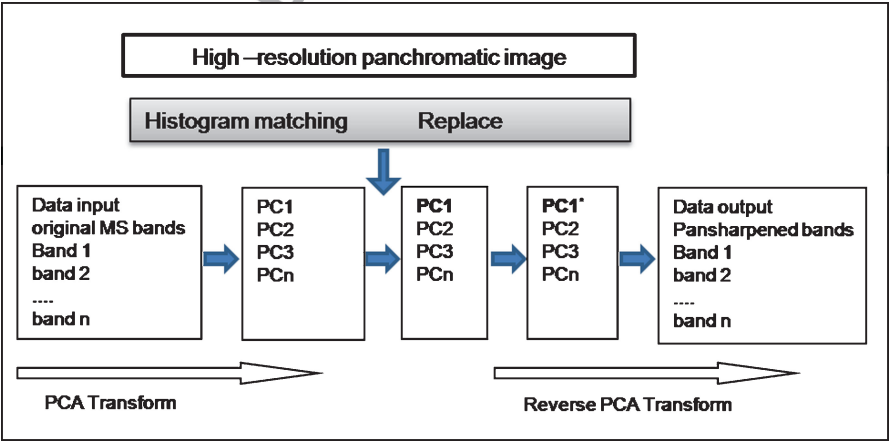


Fig. 4.4 PCA pan-sharpening scheme

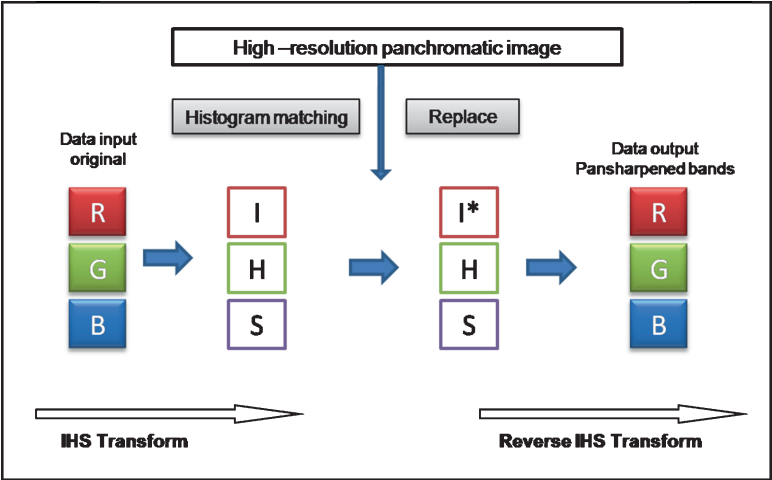


Fig. 4.5 IHS scheme

4.5.2 Intensity Hue Saturation (IHS) Pan-Sharpening

220

IHS fusion technique, originally defined for three bands only, has been extended to an arbitrary number of spectral bands (Tu et al. 2004).

The IHS transform converts a color MS image from the RGB space into the IHS color space. Because the intensity (I) band resembles a panchromatic image, it is replaced by a high-resolution Pan image in the fusion. A reverse IHS transform is then performed on the Pan together with the hue (H) and saturation (S) bands, resulting in an IHS fused image.

As for the case of pan-sharpening based on PCA, to ensure a global preservation of radiometry, the Pan band is histogram-matched to Intensity, in such a way that the two images exhibit same global mean and variance.

However, since the histogram-matched Pan image and I may not have the same local radiometry, spectral distortion, may occur and appear as local colour changes in a composition of three bands at a time. To mitigate local spectral distortion, I may be taken as a linear combination of the MS bands with weighted coefficients. These are adjusted to the overlap between the spectral response of each MS channel and that of the Pan image. In principle, if the low-pass approximation of the Pan image synthesised by combining the spectral channels exactly matches the low-resolution version of Pan, spectral distortion does not occur (Tu et al. 2004; Aiazzi et al. 2007) (Fig. 4.5).

4.5.3 Gram Schmidt

239

The Gram Schmidt (GS) pan-sharpening (Kodak / RSI patent) is based on the Gram Schmidt transformation. As PCA, this transformation rotates the original axes applying orthogonalization process to obtain a new reference system with less correlated components.

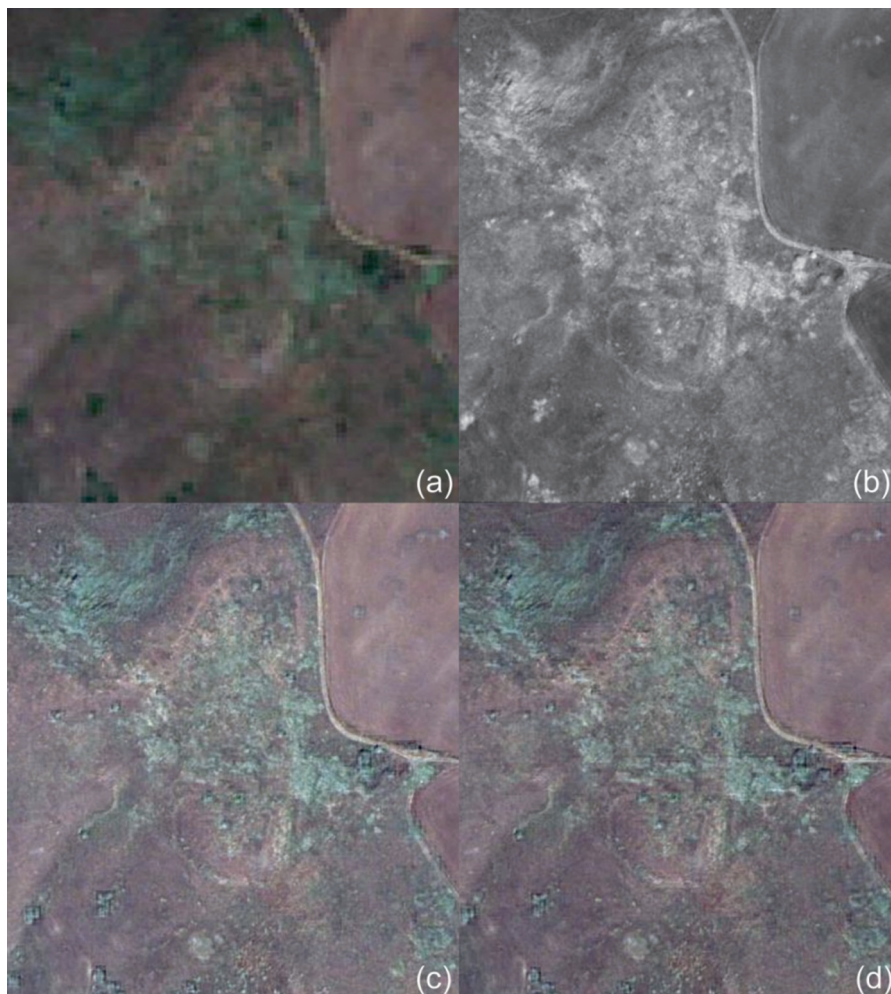


Fig. 4.6 Pan-sharpening of QuickBird multispectral images: Yrsum (Irsina, Southern Italy). (a) RGB of multispectral images; (b) Pan; (c) RGB of pan-sharpened channels by PCA method; (d) RGB of pan-sharpened channels by Gram-Schmidt method. Gram-Schmidt method allows us to discriminate the archaeological features better than PCA method

The GS approach is based on the following steps:

- (i) Pan simulation by averaging the multispectral bands;
- (ii) GS transformation using simulated Pan, assumed as the first band, and the MS bands;
- (iii) Pan replaces the first GS component;
- (iv) inverse GS transform to obtain the pan-sharpened products

Compared to PCA pan-sharpening, GS fusion products are less dependent on the dataset under processing.

Figure 4.6 shows the pan-sharpened RGB image of an archaeological site obtained by PCA e Gram Schmidt method. The latter allows us to discriminate the archaeological features better than PCA method.

4.6 Pan-Sharpening Techniques Based on Fourier Transform 255

The pan-sharpening techniques based on the Fourier Transform (Chavez et al. 1991) are based on the following computational steps:

- (I) extraction of the high frequency components from the PAN image using a high pass filter;
- (II) injection of the high frequency components into low frequency components of the multispectral images, to generate the corresponding sharpened images.

Examples of this technique are: (i) Ehlers fusion (Ehlers 2004) method which is implemented in commercial image processing ERDAS; (ii) high pass filtering techniques available as routine in the most popular image processing software such as PCI, ENVI, ERDAS.

4.6.1 Ehlers Fusion Technique 266

The Ehlers (Ehlers 2004) fusion technique is based on the following steps:

- I. IHS transform is used to separate the spatial and color information
- II. the Fourier transform, low-pass (LP) filter, is applied to intensity (obtained from the IHS transform)
- III. the Fourier transform, high-pass (HP) filter, is applied to Pan
- IV. the inverse Fast Fourier transform (FFT^{-1}), is applied both to the filtered images are converted back into the spatial domain and summed to merge the low and high frequency information derived from the coarse Intensity channel and Pan, respectively
- V. the final fused images are obtained applying the inverse IHS transformation (IHS^{-1}) (Fig. 4.7).

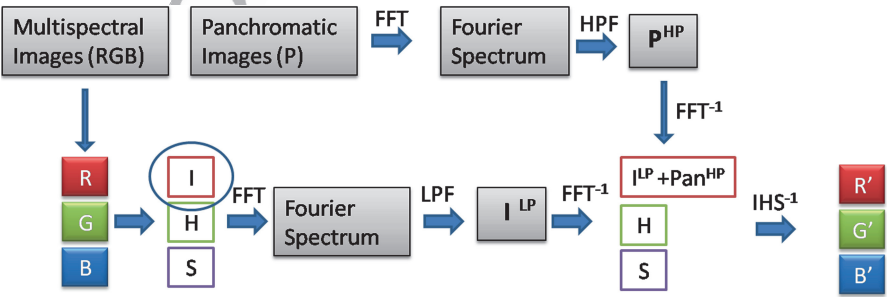


Fig. 4.7 Ehlers fusion technique scheme

278 **4.6.2 High Pass Filtering (HPF) Approach**

279 High pass filtering (HPF) pan-sharpening uses a high pass convolution filter kernel
280 whose size is generally equal to the ratio between the spatial resolution of the Pan
281 and MS images. The pan-sharpening products are obtained as follows:

- 282 (i) Pan is filtered using HPF, weighted (weights equal to kernel size) and added to
283 each multispectral band.
- 284 (ii) A linear stretch is applied to pan-sharpened products to match the mean and
285 standard deviation of MS images

286 The process may be also expressed by Eq. 4.5.

$$MS_k = \{W_{high} \cdot HF[PAN]\} \cdot \{W_{low} \cdot LF[MS'_k]\} \quad (4.5)$$

287 Where MS_k is the kth pan-sharpened image, PAN is the panchromatic image, MS'_k is
288 the original multispectral image, HF and LF correspond to the high and low pass
289 filter operators, respectively

290 High frequency components are related to the spatial detail, whereas low
291 frequency components contain spectral information.

292 The performance of these techniques depends on filtering, Kernel types, window
293 size, and weights (W_{high} and W_{low} .) which determine the amount of frequency
294 components to be combined. Generally high pass filter provide satisfactory results
295 also for multitemporal and multisensor data sets.

296 **4.7 Multi-scale Pan-Sharpening Techniques**

297 Pan-sharpening techniques based on a multiscale or multiresolution approach
298 substantially split the spatial information of the MS bands and Pan image into a
299 series of band-pass spatial frequency channels. The high frequency channels are
300 inserted into the corresponding channels of the interpolated MS bands. The sharp-
301 ened MS bands are synthesised from their new sets of spatial frequency channels.
302 Over the years a number of pan-sharpening methods based on Laplacian pyramid
303 (Núñez et al. 1999; Garzelli and Soldati 2001; Aiazzi et al. 2002). have been widely
304 used since the 1980. Recently, the use of wavelet has largely substituted the
305 Laplacian approach.

306 **4.7.1 Wavelet Transforms**

307 Recently, wavelet data analysis has become one of the fastest growing research
308 areas, being used for a number of different fields and applications, such as signal

imaging, numerical analysis, biomedical data analysis, and image processing, including image compression and reconstruction, image segmentation, pattern recognition, and satellite image fusion.

Wavelet methods transform a signal from time domain into time-frequency domain. It is evident that signal wavelet decomposition using Discrete Wavelet Transform (DWT) provides an alternative to the Discrete Fourier Transform (DFT). The main ability of DWT is the multi-resolution time-scale analysis, which is also the main advantage of DWT respect to DFT.

In the field of image processing, DWT acts in this way: an image is decomposed, with each level corresponding to a coarser resolution band.

The general scheme of the wavelet-based pan-sharpening highlights the fact that detail spatial information is extracted from the Pan image using wavelet transforms and injected into the MS image through the following three steps:

- (i) the Pan image is decomposed into a set of low-resolution images characterized by corresponding wavelet coefficients (which provide spatial details for each level);
- (ii) a MS image replaces the low-resolution Pan at the resolution level of the original MS image
- (iii) Pan spatial detail is injected into each MS band by carrying out a reverse wavelet transform using the corresponding wavelet coefficients.

Compared to other standard pan-sharpening techniques, wavelet generally performs better minimizing both color distortion and de-noising effects; nevertheless, spectral content of small objects can often be lost in the fused images. Some other general limitations are (i) the computational complexity; and (ii) the need to set up threshold values for certain parameters thus limiting the exportability to different applications, geographic regions, land cover and land use, and surface characteristics.

Pan-sharpening techniques based on DWT are implemented in many commercial image processing softwares, such as ENVI, PCI, ERDAS.

Some improved DWT, such as Ridgelet, Curvelet, and Contourlet transformation could provide better performance and results, but they have a greater computation complexity and still require setting of threshold values for given parameters (Fig. 4.8).

4.8 Artificial Neural Network

In the pan-sharpening based on Artificial Neural Networks (ANNs; additional information are in Chap. 2 Rumelhart et al. 1986; Werbos 1990) the general schematic approach can be summarized as follows:

- (i) two co-registered images are decomposed into several blocks with size of M and N;
- (ii) features of the corresponding blocks are extracted from the original Pan and MS images to obtain the normalized feature vectors;

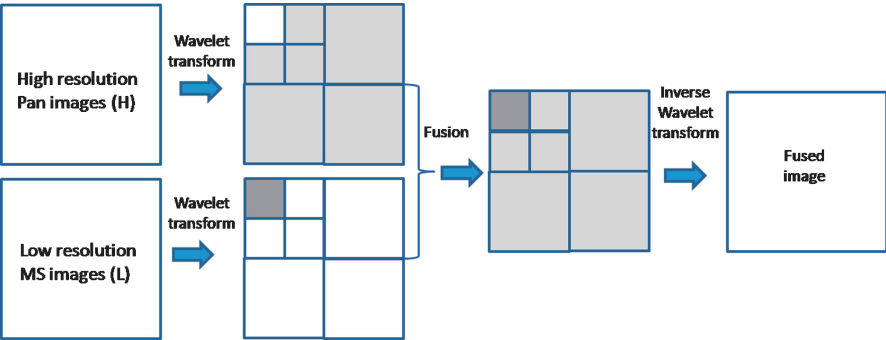


Fig. 4.8 Wavelet data fusion scheme

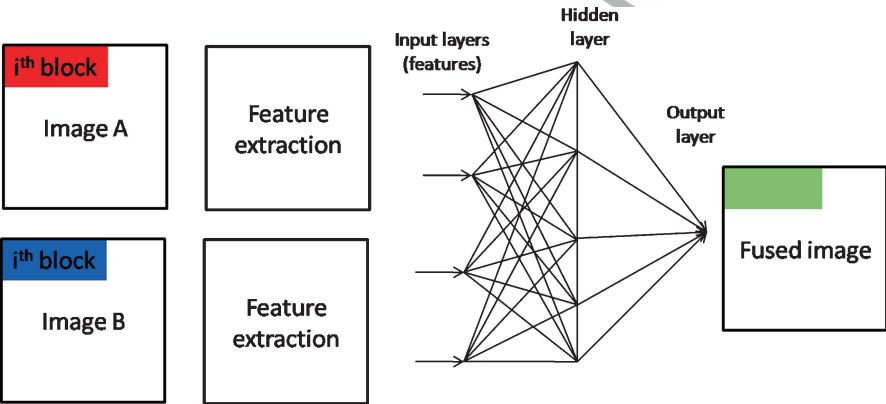


Fig. 4.9 ANN pan-sharpening scheme

348 (iii) training step is carried out from selected vector samples (Fig. 4.9).

349 The ANN pan-sharpening methods are quite efficient for high dimension data,
350 such as hyper-spectral or long-term time-series data, as well as for data from multiple
351 sensors, such as active and passive sensors, Radar and VHR satellite images. The
352 learning step of ANN can be time consuming and computationally complex.

353 **4.9 Integrated Data Fusion Approaches**

354 The most difficult aspect in data fusion is the integration of multisource remote
355 sensing data as in the case of active and passive satellite sensors. As an example,
356 fusion of SAR and optical imagery is much more difficult than the ordinary
357 pan-sharpening because the SAR data do not correlate with multispectral imagery.
358 Therefore, classical approaches of multisensor image fusion such as techniques

based on multiplication (such as Brovey transform), or component substitution (PCA, IHS) are not suitable for fusing together the spectral detail of optical data with the spatial and texture features of SAR image.

To overcome these drawbacks, feature and decision level fusion or multisource classifiers can be used (Schistad Solberg et al. 1994; Schistad Solberg et al. 1996).

In this context, wavelet multiresolution analysis has been applied successfully (Sveinsson et al. 2001; Cakir et al. 1999; Chibani and Houacine 2000; Alparone et al. 2004). For example, Alparone et al. (2004) is based on the following three steps:

- (i) extraction of SAR texture through rationing the (despeckled) SAR image with its low pass approximation,
- (ii) extraction of details from the Pan image using á trous wavelet
- (iii) high pass filtering based on modulation (HPFM) fusion method.

Wavelet transforms are one of the most widely used methods for extracting feature from multisource remote sensing data. They are also used in conjunction with other methods, such as neural network classifier.

One more example of image fusion method of optical (Pan and MS) and SAR data is in Garzelli (2002). The proposed approach is mainly based on the wavelet analysis and provides an integrated map in which selected information/features/object from SAR data are injected into the optical imagery.

4.10 Data Fusion Performance Evaluation

The assessment of the quality of the fused products is quite difficult, because no multispectral reference images are available at the requested higher spatial resolution. Over the years, several score indices or figure metrics have been devised (see, for example Thomas and Wald 2004) to evaluate the performances of the fused images. Spatial distortions (radiometric and geometric distortions) and spectral distortions (colour distortions) are generally evaluated using both intra-band indices and inter-band indices.

Wald et al. (1997) suggested that to assess the performance of data fusion algorithms, the three following properties should be fulfilled:

1. The data fusion products, once degraded to their original resolution, should be equal to the original.
2. The data fusion image should be as identical as possible to the MS image that would be acquired by the corresponding sensor with the high spatial resolution of the Pan sensor.
3. The MS set of fused images should be as identical as possible to the set of MS images that would be acquired by the corresponding sensor with the high spatial resolution of Pan.

As no multispectral reference images are available at the requested higher spatial resolution, the verification of the second and the third property is not obvious.

398 In order to overcome this drawback, these following methodological approaches
399 can be used: (i) the Wald protocol, (ii) the Zhou protocol, and, finally, (iii) the QNR
400 (Quality with No Reference) index devised by Alparone et al. (2007).

401 **4.10.1 Wald Protocol**

402 In order to solve the problems linked to the unavailability of the multispectral
403 reference images, Wald et al. (1997) suggested a protocol to be applied in order to
404 evaluate the quality of data fusion products. Such a protocol is based on the
405 following three steps:

- 406 1. spatial degradation of both the Pan and MS images by the same factor,
- 407 2. fusing the MS images at the degraded scale;
- 408 3. comparing the fused MS images with the original reference MS images.

409 The Wald protocol assumes a scale invariance behaviour.

410 This means that performances of fusion methods are supposed to be invariant
411 when fusion algorithms are applied to the full spatial resolution. Nevertheless, in the
412 context of remote sensing of archaeology, the small features, which represent a large
413 amount of the archaeological heritage, can be lost after degrading both the Pan and
414 MS. In these situations, the archaeological features will be missed, and, therefore, the
415 evaluation of data fusion results could not be performed over the targets of interest.

416 **4.10.2 Zhou Protocol**

417 As an alternative to the Wald's protocol, the problem of measuring the fusion quality
418 may be approached at the full spatial scale without any degradation by applying
419 Zhou's Protocol (Zhou et al. 1998). Such a protocol is based on the following three
420 criteria:

- 421 (1) Both the spectral and spatial qualities are evaluated, but by using separate
422 scores from the available data: the first from the low resolution MS bands and
423 the second one from the high resolution Pan image.
- 424 (2) The evaluation of spectral quality is performed for each band by computing an
425 absolute cumulative difference between the fused and the input MS images.
- 426 (3) The evaluation of spatial quality is obtained as the correlation coefficient (CC)
427 computed between the spatial details of the Pan image and of each of the fused
428 MS bands.

429 Such spatial details are extracted by using a Laplacian filter. Unfortunately,
430 some problems can arise by using Zhou's Protocol (Alparone et al. 2007). Firstly,
431 the two quality measures follow opposite trends. Secondly, at degraded scale, the
432 obtained results cannot be in agreement with objective quality indices.

4.10.3 QNR Index

433

The QNR (Quality with No Reference) index devised by Alparone et al. (2007) is a “blind” index capable of jointly measuring the spectral and spatial quality at the full scale. This index should allow to overcome the drawbacks that can arise when using Zhou’s protocol.

The QNR computes both the spatial and spectral distortion from the quality index (Q) by Wang and Bovik (2002).

This index combines the correlation coefficient with luminance and contrast distortion. It was devised for image fusion to assess the quality of output image, as well as for evaluating image processing systems and algorithms. Given an image X and its reference image Y , the quality index proposed by Wang and Bovik (2002) is calculated as:

$$Q = \frac{(2\mu_x + \mu_y + C_1)(2\sigma_{xy} + C_2)}{(\mu_x^2 + \mu_y^2 + C_1)(\sigma_x^2 + \sigma_y^2 + C_2)} \quad (4.6)$$

Where $C_1 = (k_1L)$ and $C_2 = (k_2L)$, μ_x and μ_y indicate the mean of the two images X and its reference image Y , σ_x and σ_y are the standard deviation, σ_{xy} represents the covariance between the two images, and L is the dynamic range for the image pixel values, $k_1 \ll 1$ and $k_2 \ll 1$ are two constants chosen equal to 0.01 and 0.03, respectively.

Although the values selected for k_1 and k_2 are arbitrary, it was experienced that the quality index is insensitive to variations of k_1 and k_2 . Note that C_1 and C_2 are solely introduced to stabilize the measure. In other word, just to avoid the denominator approaches zero values for flat regions.

To measure the overall image quality the mean quality index can be rewritten as a three factor product, that can be regarded are relatively independent.

$$Q(x, y) = f(l(x, y), c(x, y), s(x, y)) \\ = \frac{(\sigma_{xy} + C_3)}{(\sigma_x\sigma_y + C_3)} \frac{(2\mu_x\mu_y + C_1)}{(\mu_x^2 + \mu_y^2 + C_1)} \frac{(2\sigma_x\sigma_y + C_2)}{(\sigma_x^2 + \sigma_y^2 + C_2)} \quad (4.7)$$

where C_3 is a small positive constants as C_1 and C_2 .

In particular, among the three factor of Eq. 4.2, the first (varying between -1 and 1) represents the correlation coefficient between the two image x and y ; the second (varying between 0 and 1) measures the similarity between the mean luminance values of x and Y , and finally, the third (varying between 0 and 1) measures the contrast similarity.

The rationale The QNR (Quality with No Reference) index devised by Alparone et al. (2007) is that the Q index calculated between any two spectral bands and between each band and the Pan image should be unchanged after fusion. In order to obtain a single index, both the spectral and spatial distortion indices are

466 complemented and combined together to obtain a single index that measures the
467 global quality of the fused image.

468 In detail, the spectral distortion is computed as follows:

469 The spectral distortion is obtained by computing the difference of Q values from
470 the fused MS bands and the input MS bands, re-sampled at the same spatial
471 resolution as the Pan image

472 The Q is calculated for each couple of bands of the fused and re-sampled MS
473 data to form two matrices with main diagonal equal to 1

474 The measure of spectral distortion DI is computed by using a value proportional
475 to the p -norm of the difference of the two matrices.

$$D_{\lambda} = \sqrt[p]{\frac{1}{L^2 - L} \sum_{l=1}^L \sum_{\substack{r=1 \\ r \neq l}}^L |Q(\hat{G}_e, \hat{G}_r) - Q(\tilde{G}_e, \tilde{G}_r)|^2} \quad (4.8)$$

476 where L is the number of the spectral bands processed, and $Q(\hat{G}_e, \hat{G}_r)$ denotes that
477 Q is calculated for each couple of bands of the fused and resampled MS data.

478 The spatial distortion is computed two times: (1) between each fused MS band
479 and the Pan image; and than (2) between each input MS band and the spatially
480 degraded Pan image. The spatial distortions D_s are calculated by a value propor-
481 tional to the q -norm of the differences

$$D_s = \sqrt[q]{\frac{1}{L} \sum_{l=1}^L |Q_n(\hat{G}_l, P) - Q_n(\tilde{G}_l, \tilde{P})|^q} \quad (4.9)$$

482 where L is the number of the spectral bands processed, and \hat{G}_l, P denotes the Q is
483 calculated between each fused MS band and the Pan image, and $Q_n(\hat{G}_l, P)$ denotes the
484 Q is calculated between each input MS band and the spatially degraded Pan image.

485 Just as an example, we refer to an application related to an archaeological site in
486 Southern Italy (Lasaponara et al. 2007). It is Metaponto which was before a Greek
487 colony (700 BC–200 BC), then it was frequented by Romans (200 BC–400 AD).

488 QuickBird imagery has been used to identify and study linear features which
489 have been thought to ancient field divisions or other features of archaeological
490 interest. Such features are better visible from NIR channel respect to other channels.
491 To improve the details pan-sharpening has been carried out by using Gram
492 Schmidt, PCA and Wavelet Transform methods.

493 The NIR pan-sharpened products (Fig. 4.10) have been compared by visual
494 inspection by about ten colleagues including experts of remote sensing,
495 archaeologists and geophysicists. According the involved researchers Wavelet
496 pan-sharpening provides the best result in terms of visibility of archaeological
497 features.



Fig. 4.10 Visualization of NIR pan-sharpened images obtained by using Gram Schmidt (*upper*), PCA (*medium*) and Wavelet transform (*lower*) methods

t1.1 **Table 4.1** Evaluation of three pan-sharpening NIR channels by using the Wald and Alparone protocols

t1.2	t1.3	Wald protocol Bovik score index				Alparone protocol QNR score index
		I component	II component	III component	Q	
t1.4	Gram Schmidt	0.508	0.999	0.506	0.257	0.632
t1.5	PCA	0.727	0.886	0.640	0.413	0.673
t1.6	Wavelet	0.773	0.999	0.769	0.595	0.863

498 Then the same pan-sharpened dataset has been evaluated in a quantitative way
499 by applying the Wald and Alparone protocols. For both of them the best perfor-
500 mance was clearly achieved by using the wavelet-based data fusion (see Table 4.1).

501 **4.11 Final Remarks**

502 This chapter is composed of two parts, the first provided an overview of diverse
503 pan-sharpening techniques; whereas, the second part focused on the protocols
504 available for the numerical evaluation of performance.

505 The most common used methods are described in detail. In particular, we focused
506 the different methodological approaches, such as pan-sharpening techniques based
507 on: (i) arithmetic combinations (among them Multiplicative approach, Brovey trans-
508 formation, SVR); (ii) component Substitution (among them HIS, PCA and Gram-
509 Schmidt); (iii) Fourier Transform (Ehlers, HPF); (iv) Multiscale/multiresolution
510 (wavelet, Laplacian); (v) Artificial Neural Networks.

511 The simplest approach is the arithmetic combination of different scenes
512 performed at the pixel level. The CS fusion method is based on diverse types of
513 transformations which are applied to synthesise a Pan image, later substituted by the
514 real pan and, finally, the application of the reverse transformation provides the
515 fused products. The pan-sharpening techniques based on the Fourier Transform
516 extract the high frequency components from the PAN image (using a high pass
517 filter) and inject them into low frequency components of the multispectral images.
518 Multiscale/multiresolution approaches split the spatial information of the MS bands
519 and Pan image into a series of band-pass spatial frequency channels. The high
520 frequency channels are inserted into the corresponding channels of the interpolated
521 MS bands. In the pan-sharpening based on Artificial Neural Networks the images
522 are firstly decomposed into several blocks, later features are extracted from the
523 original Pan and MS scene and finally the training step is carried out.

524 Moreover we also highlighted the protocols in use for the numerical comparison
525 and evaluation of different approaches, in terms of spectral fidelity and spatial
526 resolution performance.

The visual inspection is not enough to compare results obtained from different algorithms but automatic quality assessment is highly desirable to evaluate performance and benefits of Pan-sharpening techniques. Considering that archaeological features are characterized by quite subtle signals, It clearly shows that the quantitative evaluation of performance from pan-sharpening methods is a critical issue for archaeological applications.

Nowadays, several mathematical methods have been adopted to evaluate the quality of merged imagery (i) Specific protocols for quality measures such as well as (ii) Statistical indices, such as cross entropy, mean square error, and signal-to-noise ratio. Nevertheless, up to now analytical studies of these measures are still lacking. New performance assessment criteria and automatic quality assessment methods will be addressed in future research.

Moreover, specific context-adaptive indices need to be developed, because outputs from the existing evaluation procedures cannot fit the specific requirement of cultural features sharpening. Although the application of pan-sharpening techniques for enhancing cultural features is a quite recent topic, we would like to point out their potentiality for improving the identification of unknown archaeological buried structures.

References

- Aiazzi B, Alparone L, Baronti S, Garzelli A (2002) Context-driven fusion of high spatial and spectral resolution data based on oversampled multiresolution analysis. *IEEE Trans Geosci Remote Sens* 40(10):2300–2312
- Aiazzi B, Baronti S, Selva M (2007) Improving component substitution pan-sharpening through multivariate regression of MS + PAN data. *IEEE Trans Geosci Remote Sens* 45(10):3230–3239
- Aiazzi B, Baronti S, Alparone L, Lasaponara R, Masini N (2008) Data fusion techniques for supporting and improving satellite-based archaeological research. In: Lasaponara R, Masini N (eds) *Advances in remote sensing for archaeology and cultural heritage management*. Aracne, Roma, pp 31–36
- Alparone L, Baronti S, Garzelli A, Nencini F (2004) Landsat ETM + and SAR image fusion based on generalized intensity modulation. *IEEE Trans Geosci Remote Sens* 42:2832–2839
- Alparone L, Aiazzi B, Baronti S, Selva M, Garzelli A, Nencini F (2007) Quality assessment without reference of pan-sharpened MS images. In: *Proceedings of EARSel symposium 5–7 June 2007*, Bozen
- Cakir HJ, Khorram S, Dai XL, de Fraipont P (1999) Merging SPOT XS and SAR imagery using the wavelet transform method to improve classification accuracy. In: *Geoscience and remote sensing symposium. IGARSS '99 proceedings, IEEE 1999 International*, 28 June–2 July 1999
- Chavez PS Jr, Sides SC, Anderson JA (1991) Comparison of three different methods to merge multiresolution and multispectral data: Landsat TM and SPOT panchromatic. *Photogramm Eng Remote Sens* 57(3):295–303
- Chibani Y, Houacine A (2000) On the use of the redundant wavelet transform for multisensor image fusion. In: *Proceedings of the 7th IEEE international conference on electronics, circuits and systems*, Lebanon, 17–20 Dec 2000. *ICECS 2000*, vol 1, pp 442–445
- Dong J, Zhuang D, Huang Y, Jingying Fu (2009) *Advances in multi-sensor data fusion: algorithms and applications*. *Sensors* 9:7771–7784

- 572 Ehlers M (2004) Spectral characteristics preserving image fusion based on Fourier domain
573 filtering. In: Ehlers M, Kaufmann HJ, Michel U (eds) Remote sensing for environmental
574 monitoring, GIS applications, and geology IV. Proceedings of SPIE, Bellingham, pp 1–13
- 575 Garzelli A (2002) Possibilities and limitations of the use of wavelets in image fusion. In:
576 Proceedings of the IEEE international geoscience and remote sensing symposium, Toronto,
577 24–28 June 2002. IGARRS 02, vol 1, pp 66–68.
- 578 Garzelli A, Soldati F (2001) Context-driven image fusion of multispectral and panchromatic data
579 based on a redundant wavelet representation. In: Proceedings of the IEEE/ISPRS joint work-
580 shop on remote sensing and data fusion over urban areas, Rome, 8–9 Nov 2001, pp 122–126
- 581 Laben CA, Bernard V, Brower W (2000) Process for enhancing the spatial resolution of multi-
582 spectral imagery using pan-sharpening. US Patent 6,011,875
- 583 Lasaponara R, Masini N (2007) Detection of archaeological crop marks by using satellite
584 QuickBird multispectral imagery. *J Archaeol Sci* 34:214–221
- 585 Lasaponara R, Lanorte A, Coluzzi R, Masini N (2007) Performance evaluation of data fusion
586 techniques for archaeological prospection based on satellite data. In: Proceedings of SPIE,
587 vol 6749, 67492W. doi: 10.1117/12.738204
- 588 Lasaponara R, Masini N, Aiazzi B, Alparone L, Baronti S (2008) Satellite-based enhancement of
589 archaeological marks through data fusion techniques. In: Proceedings of the SPIE, vol 7110,
590 711024. doi:10.1117/12.801569
- 591 Munechika CK, Warnick JS, Salvaggio C, Schott JR (1993) Resolution enhancement of multi-
592 spectral image data to improve classification accuracy. *Photogramm Eng Remote Sens* 59(1):
593 67–72
- 594 Núñez E, Otazu X, Fors O, Prades A, Palà V, Arbiol R (1999) Multiresolution-based image fusion
595 with adaptive wavelet decomposition. *IEEE Trans Geosci Remote Sens* 37(3):1204–1211
- 596 Pohl C, Van Genderen JL (1998) Multisensor image fusion in remote sensing: concepts, methods
597 and applications. *Int J Remote Sens* 19:823–854
- 598 Richards JA, Jia X (2006) Remote sensing digital image analysis. Hardback, 4th edn. Springer,
599 Berlin/Heidelberg, 476 p
- 600 Rumelhart D, Hinton G, Williams R (1986) Learning internal representations by error propagation.
601 In: McClelland JL, Rumelhart DE, The PDP Research Group (eds) Parallel distributed
602 processing: explorations in the microstructure of cognition. The MIT Press, Cambridge,
603 vol 1, pp 318–362
- 604 Schistad Solberg AH, Jain AK, Taxt T (1994) Multisource classification of remotely sensed data:
605 fusion of Landsat TM and SAR images. *IEEE Trans Geosci Remote Sens* 32(4):768–778
- 606 Schistad Solberg AH, Taxt T, Jain AK (1996) A markov random field model for classification of
607 multisource satellite imagery. *IEEE Trans Geosci Remote Sens* 34(1):100–113
- 608 Suits G, Malila W, Weller T (1988) Procedures for using signals from one sensor as substitutes for
609 signals of another. *Remote Sens Environ* 25:395–408
- 610 Sveinsson JR, Ulfarsson MO, Benediktsson JA (2001) Cluster-based feature extraction and data
611 fusion in the wavelet domain. In: Geoscience and remote sensing symposium, 2001. IGARSS
612 '01. IEEE 2001 International, vol 2, 9–13 July 2001, pp 867–869
- 613 Thomas C, Wald L (2004) Assessment of the quality of fused products. In: Oluic M (ed)
614 Proceedings of 24th EARSeL Symposium on New Strategies for European Remote Sensing,
615 Dubrovnik, 25–27 May 2004. Balkema, Rotterdam, pp 317–325
- 616 Tu TM, Huang PS, Hung CL, Chang C-P (2004) A fast intensity-hue-saturation fusion technique
617 with spectral adjustment for IKONOS imagery. *IEEE Trans Geosci Remote Sens* 42(4):309–312
- 618 Wald L, Ranchin T, Mangolini M (1997) Fusion of satellite images of different spatial resolutions:
619 assessing the quality of resulting images. *Photogramm Eng Remote Sens* 63(6):691–699
- 620 Wang Z, Bovik AC (2002) A universal image quality index. *IEEE Signal Proc Lett* 9(3):81–84
- 621 Wang L, Cao X, Chen J (2008) ISVR: an improved synthetic variable ratio method for image
622 fusion. *Geocarto Int* 23(2):155–165

- Werbos PJ (1990) Backpropagation through time: what it does and how to do it. *Proc IEEE* 623
78:1550–1560 624
- Zhang Y (2004) Understanding image fusion. *Photogramm Eng Rem Sens* 70:657–661 625
- Zhou J, Civco DL, Silander JA (1998) A wavelet transform method to merge Landsat TM and 626
SPOT panchromatic data. *Int J Remote Sens* 19(4):743–757 627

